Critical Fluorescence of a Transmon at the Schmid Transition

M. Houzet[1] and L. I. Glazman[2]
[1]Univ. Grenoble Alpes, CEA, IRIG, PHELIQS, 38000 Grenoble, France
[2]Departments of Physics and Applied Physics, Yale University, New Haven, Connecticut 06520, USA

(Received 5 September 2020; accepted 3 December 2020; published 30 December 2020)

We investigate inelastic microwave photon scattering by a transmon qubit embedded in a high-impedance circuit. The transmon undergoes a charge-localization (Schmid) transition upon the impedance reaching the critical value. Because of the unique transmon level structure, the fluorescence spectrum carries a signature of the transition point. At higher circuit impedance, quasielastic photon scattering may account for the main part of the inelastic scattering cross section; we find its dependence on the qubit and circuit parameters.

DOI: 10.1103/PhysRevLett.125.267701

Introduction.—A quantum-mechanical degree of freedom can be severely affected by its coupling to a dissipative environment. In a pioneering work [1], Schmid predicted that a superconducting circuit as elementary as a Josephson junction is insulating when it is Ohmically shunted by a resistance larger than the resistance quantum, $R_Q = \pi\hbar/2e^2$. This result, which was further studied in Refs. [2–4], reflects a charge localization transition, which is associated with the breaking of the ground state degeneracy. Remarkably the prediction holds at any ratio between the Josephson and charging energies of the junction, $\tilde{E}_J$ and $\tilde{E}_C = e^2/2\tilde{C}$, respectively, where $\tilde{C}$ is the junction capacitance [5]. So far evidence for the charge localization transition by dc [6–8] or low-frequency [9] measurements remains elusive.

As a quantum many-body effect, the Schmid transition should not only affect the ground state, but the excited states as well. Here we find a spectroscopic signature of the transition in the fluorescence spectrum [10] of a weakly nonlinear Josephson junction with $\tilde{E}_C \ll \tilde{E}_J$, a.k.a. a transmon qubit [12,13], coupled to a Josephson-junction chain. The chain realizes a transmission line with an adjustable impedance [14,15], in which plasmon waves or, equivalently, microwave photons propagate freely. This setup attracted recent experimental interest [16–18] as a way to emulate quantum impurity problems with superconducting quantum circuits [19–24]. Our theory predicts a characteristic dependence of the inelastic scattering cross sections on the parameters of the setup.

Model.—Our consideration starts with the superconducting circuit of Fig. 1. The Josephson-junction chain to which the transmon is coupled is characterized by the Josephson energy E_J, and charging energies $E_C = e^2/2C$ and $E_g = e^2/2C_g$, where C and C_g are the chain's junction and ground capacitances. Under the conditions

$$E_C E_J \gg \tilde{E}_C \tilde{E}_J \gg \tilde{E}_C^2, \tag{1}$$

the classical analysis, in which the Josephson junctions are approximated as linear inductances, yields a narrow transmon resonance that lies deep in the linear part of the waves' dispersion. The transmon resonance frequency and half-width are, respectively, $\omega_0 = \sqrt{8\tilde{E}_C\tilde{E}_J}/\hbar$ and $\Gamma = 1/2Z\tilde{C}$; the waves' dispersion is $\omega_p = vp/\sqrt{(vp/\omega_B)^2 + 1}$. Here $Z = R_Q/2K$ with $K = \pi\sqrt{E_J/8E_g}$ is the chain's impedance at low frequency, $\omega_B = \sqrt{8E_CE_J}/\hbar$ is the photon bandwidth, $v = a\sqrt{8E_JE_g}/\hbar$ is the photon velocity and a is the chain's unit cell length. Noting that $\Gamma = (4/\pi\hbar)K\tilde{E}_C$ and assuming $K \lesssim 1$ in the relevant range of parameters, we find from Eq. (1) that, indeed, $\Gamma \ll \omega_0 \ll \omega_B$. Within the classical analysis, photon scattering is purely elastic.

To analyze inelastic scattering, we first notice that $K = 1/2$ is the critical value for the Schmid transition [1]. Below that value, the environment induces charge localization. The elementary processes responsible for it are phase slips [25]. In an isolated transmon, the phase slip amplitude for the first excited band is [12]

$$\lambda_1 = \frac{64}{\sqrt{\pi}}\frac{\tilde{E}_C}{\hbar}\left(\frac{2\tilde{E}_J}{\tilde{E}_C}\right)^{5/4} e^{-\sqrt{8\tilde{E}_J/\tilde{E}_C}} \tag{2}$$

(parametrically larger than the phase slip amplitude for the ground state, $\lambda_1/\lambda_0 = -8\sqrt{2\tilde{E}_J/\tilde{E}_C}$). Therefore, Γ may

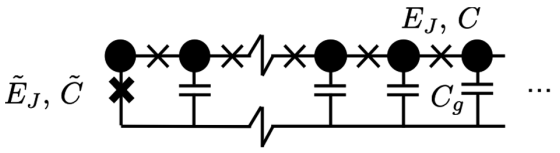

FIG. 1. We study microwave photon scattering off a transmon coupled to a Josephson-junction chain. The transmon has Josephson energy $\tilde{E}_J$ and capacitance $\tilde{C}$. The junctions in the chain have Josephson energy E_J and capacitance C, each superconducting island has ground capacitance C_g.

become parametrically smaller than λ_1 *only* deep in the localized regime, $K \ll 1$. Barring that, we treat phase slips perturbatively. In most of the discussion below we assume $\lambda_1 \ll \Gamma$. At the same time, the proliferation of phase slips in the chain's junctions, with an amplitude $\lambda_{\rm chain} \propto e^{-\sqrt{8E_J/E_C}}$, is known to drive a superfluid-to-insulating transition below the critical value $K = 2$ [26–28]. That physics can be disregarded either if the bandwidth Γ that limits frequency exchange in a quasielastic process (see below) is larger than the insulating gap, $\Gamma \gg \lambda_{\rm chain}$, or if the chain is short enough to evade the thermodynamic limit, $L < v/\lambda_{\rm chain}$ (but still long enough to ignore effects related to a finite level spacing, $\Delta = \pi v/L \to 0$).

Ignoring the chain's nonlinearity we use Hamiltonian

$$H = 4\tilde{E}_C(\hat{N} - \hat{n})^2 + \tilde{E}_J[1 - \cos\hat{\varphi}] + \sum_p \hbar\omega_p a_p^\dagger a_p \tag{3}$$

to describe the setup. Here $\hat{\varphi}$ and $\hat{N}$ are the transmon's conjugate phase and charge operators, a_p and $a_p^\dagger$ are the annihilation and creation operators of a linearly dispersing photon of wave vector p, and

$$\hat{n} = \frac{1}{\pi}\sum_{p>0} f_p(a_p + a_p^\dagger) \quad \text{with} \quad f_p = \sqrt{K\Delta/\omega_p} \tag{4}$$

is the charge displacement operator at the qubit. The sum in Eq. (4) includes only the dynamical variables of the chain. The static mode ($p = 0$) compensates for an eventual charge offset, which is effectively attenuated by the total capacitance of the array, $\sim C_g \cdot (L/a)$ [29].

The low-energy properties of Eq. (3) are described by the boundary sine-Gordon model, $H_{\rm sG} = \sum_p \hbar\omega_p a_p^\dagger a_p - \lambda_0 \cos(2\pi\hat{n})$ [30]. Keeping the ratio $\tilde{E}_C/\tilde{E}_J$ small but finite generalizes it to a new quantum impurity problem, in which the transmon resonance brings in a nontrivial structure of the high-frequency spectrum, as we discuss now.

Phase-slip vs quartic anharmonicities.—We first show, by perturbative analysis in coupling f_p, that phase slips play the dominant role in quasielastic (or soft) photon scattering, i.e., inelastic scattering with a small energy transfer between the incoming and one of the outgoing photons. For this we write the Hamiltonian (3) in the transmon basis of discrete eigenstates (we set $\hbar = 1$ hereinafter),

$$H = H_0 + V, \quad H_0 = \sum_s \varepsilon_s |s\rangle\langle s| + \sum_p \omega_p a_p^\dagger a_p + 4E_C\hat{n}^2,$$
$$V = -\hat{n}\sum_{ss'} W_{ss'}|s\rangle\langle s'| \quad \text{with} \quad W_{ss'} = 8E_C\langle s|\hat{N}|s'\rangle. \tag{5}$$

Here we ordered the transmon eigenenergies, $\varepsilon_s > \varepsilon_{s'}$ if $s > s' \geq 0$, and set $\varepsilon_0 = 0$. The partial inelastic cross section for a photon with frequency ω to be converted into three photons with frequencies ω_1, ω_2, ω_3, such that $\omega = \omega_1 + \omega_2 + \omega_3$, is obtained with Fermi's golden rule,

$$\gamma(\omega_1, \omega_2, \omega_3|\omega) = \frac{2\pi^2}{3!}\frac{|\mathcal{A}_{p;p_1p_2p_3}|^2}{\Delta^4} \tag{6}$$

(3! accounts for permutations of momenta that describe the same final state) with $\omega = \omega_p$, $\omega_i = \omega_{p_i}$, and a matrix element obtained perturbatively in f_p,

$$\begin{aligned}\mathcal{A}_{p;p_1p_2p_3} &= \langle 0|a_{p_1}a_{p_2}a_{p_3}V\left(\frac{1}{\omega_p - H_0}V\right)^3 a_p^\dagger|0\rangle \\ &= -\frac{K^2\Delta^2}{\pi^4\sqrt{\omega\omega_1\omega_2\omega_3}}\sum_{srt} W_{0s}W_{sr}W_{rt}W_{t0} \\ &\times\Bigg\{\frac{1}{(\varepsilon_s+\omega_1+\omega_2-\omega)(\varepsilon_r+\omega_1-\omega)(\varepsilon_t-\omega)} \\ &+\frac{1}{(\varepsilon_s+\omega_1+\omega_2-\omega)(\varepsilon_r+\omega_1-\omega)(\varepsilon_t+\omega_1)} \\ &+\frac{1}{(\varepsilon_s+\omega_1+\omega_2-\omega)(\varepsilon_r+\omega_1+\omega_2)(\varepsilon_t+\omega_1)} \\ &+\frac{1}{(\varepsilon_s+\omega_1+\omega_2+\omega_3)(\varepsilon_r+\omega_1+\omega_2)(\varepsilon_t+\omega_1)} \\ &+\text{permutations of } \omega_1,\omega_2,\omega_3.\Bigg\}\end{aligned} \tag{7}$$

Here we ignored the last term in H_0 (it vanishes in the thermodynamic limit), and the summation is over the transmon levels. The most divergent terms correspond to the following sequences of transmon virtual states, $0 \to 1 \to 0 \to t \to 0$, $0 \to 1 \to r \to 1 \to 0$, or $0 \to s \to 0 \to 1 \to 0$, and to frequencies such that

$$|\omega - \varepsilon_1|, |\omega_1 - \varepsilon_1|, \omega_2, \omega_3 \ll \varepsilon_1 \tag{8}$$

(as well as two other inequalities after permutation of ω_1, ω_2, ω_3). The contribution to $\mathcal{A}_{p;p_1p_2p_3}$ that corresponds to the on-shell condition, $\omega = \omega_1 + \omega_2 + \omega_3$, and satisfies the inequalities (8), is

$$-\frac{2K^2\Delta^2}{\pi^4\varepsilon_1\sqrt{\omega_2\omega_3}}\frac{|W_{01}|^2}{(\omega-\varepsilon_1)(\omega_1-\varepsilon_1)}\sum_s\left(\frac{|W_{1s}|^2}{\varepsilon_s-\varepsilon_1} - \frac{|W_{0s}|^2}{\varepsilon_s}\right). \tag{9}$$

By substituting the operator $\hat{n}$ with a gate charge $\mathcal{N}$ in Eq. (5), one can calculate the gate sensitivity of the energy levels $\varepsilon_{1,0}(\mathcal{N})$ perturbatively in $\mathcal{N}$, and identify [31]

$$\sum_s\left(\frac{|W_{1s}|^2}{\varepsilon_s-\varepsilon_1} - \frac{|W_{0s}|^2}{\varepsilon_s}\right) = \frac{1}{2}\frac{\partial^2[\varepsilon_1(\mathcal{N}) - \varepsilon_0(\mathcal{N})]}{\partial\mathcal{N}^2}\bigg|_{\mathcal{N}=0}. \tag{10}$$

In the transmon limit [cf. Eqs. (1) and (2)], $\varepsilon_s(\mathcal{N}) = \varepsilon_s(1/4) + \lambda_s\cos(2\pi\mathcal{N})$, allowing us to replace the right-hand

side of the exact Eq. (10) with $2\pi^2(\lambda_1-\lambda_0)\approx 2\pi^2\lambda_1$. Evaluating all remaining factors in Eq. (9) within the transmon's harmonic approximation, in which $\varepsilon_s^{(0)}\approx s\omega_0$ and $W_{sr}^{(0)}=8\tilde{E}_C(\tilde{E}_J/32\tilde{E}_C)^{1/4}[\sqrt{s}\delta_{s,r+1}+\sqrt{s+1}\delta_{s,r-1}]$, we find the leading quasielastic [or soft inelastic (si)] contribution to Eq. (6) for frequencies satisfying the conditions (8),

$$\gamma_{\rm si}(\omega_1,\omega_2,\omega_3|\omega)=\frac{16}{3}\frac{K^2\Gamma^2\lambda_1^2}{\omega_2\omega_3(\omega_1-\omega_0)^2(\omega-\omega_0)^2}. \quad (11)$$

The partial cross section of quasielastic scattering, which characterizes the transmon fluorescence,

$$\gamma_{\rm si}(\omega'|\omega)=\int_0^{\omega-\omega'}d\omega_2\gamma_{\rm si}(\omega',\omega_2,\omega-\omega'-\omega_2|\omega), \quad (12)$$

is obtained at $|\omega-\omega_0|,|\omega'-\omega_0|\ll\omega_0$ from Eq. (11), and two other equations with permutations of ω_1, ω_2, ω_3, as

$$\gamma_{\rm si}(\omega'|\omega)=\frac{32K^2\Gamma^2\lambda_1^2}{(\omega-\omega_0)^2(\omega'-\omega_0)^2(\omega-\omega')}\ln\left(\frac{\omega-\omega'}{\Delta}\right); \quad (13)$$

here we used Δ as a low-frequency cutoff.

We contrast Eq. (13) with the one obtained for a weak anharmonic (quartic) oscillator, after approximating $1-\cos\varphi\approx\varphi^2/2-\varphi^4/24$ in the Josephson term of Eq. (3) and neglecting the phase slips. In that case, the gate sensitivity is absent, the right-hand side of the identity (10) is zero, rendering $\gamma_{\rm si}(\omega'|\omega)=0$. In harmonic approximation, Eq. (7) vanishes identically. Treating the anharmonic corrections to ε_s and W_{sr} appearing in Eq. (7) perturbatively, and assuming the incident photon to be close to resonance, $|\omega-\omega_0|\ll\omega_0$, yields

$$\gamma_{\rm q}(\omega_1,\omega_2,\omega_3|\omega)=\frac{(256/3\pi^2)\Gamma^4\tilde{E}_C^2\omega_0^3\omega_1\omega_2\omega_3}{[(\omega_0-\omega)(\omega_0^2-\omega_1^2)(\omega_0^2-\omega_2^2)(\omega_0^2-\omega_3^2)]^2}. \quad (14)$$

Assuming that the outgoing photon is also close to resonance, $|\omega'-\omega_0|\ll\omega_0$, we get

$$\gamma_{\rm q}(\omega'|\omega)=\frac{32}{9\pi^2}\frac{\Gamma^4\tilde{E}_C^2(\omega-\omega')^3}{\omega_0^6(\omega-\omega_0)^2(\omega'-\omega_0)^2}. \quad (15)$$

The comparison of Eqs. (13) and (15) shows that phase slips are much more effective in coupling the resonant modes to the low-frequency ones than the anharmonic corrections to the qubit levels. The low-frequency modes, being far away from the resonance, do not hybridize well with the qubit. The phase slips are free from that drawback (at the expense of a potentially small value of λ_1). Thus phase slips dominate in the inelastic processes at $\omega'\to\omega$.

Differential cross section.—We proceed further by accounting for higher-order quasielastic processes at finite K. The dichotomy between the high-frequency photon modes that are in resonance with the transmon and the low-frequency modes motivates a two-band approximation:

$$H_{\rm eff}=\omega_0|1\rangle\langle 1|+\sum_{p>p_c}\omega_p|p\rangle\langle p|+\sum_{p>p_c}[t|p\rangle\langle 1|+{\rm H.c.}] + \sum_{0<p<p_c}\omega_p a_p^\dagger a_p+\lambda_1|1\rangle\langle 1|\cos(2\pi\tilde{n}). \quad (16)$$

Here the first line represents the hybridization of the transmon with high-frequency photons; $|p\rangle=a_p^\dagger|0\rangle$, where $|0\rangle$ is the ground state, $|1\rangle$ is the state in which (only) the transmon is excited, and $t=\sqrt{\Gamma\Delta/\pi}$ is the hybridization matrix element. The second line in Eq. (16) accounts for the coupling of low-frequency photons and the transmon excited state through phase slips [32]; the local charge operator $\tilde{n}$ differs from Eq. (4) by the restriction of the sum to low-frequency modes, $0<p<p_c$. The separation between low- and high-frequency photons is set by frequency $\omega_c=vp_c$, such that $\Gamma\ll\omega_0-\omega_c\ll\omega_0$.

The first line in the Hamiltonian (16) is equivalent to the Fano-Anderson model. Its eigenstate $|k\rangle$ with energy ω_k such that $\omega_k-\omega_0=-\Gamma\tan(\omega_kL/v)$ has an overlap

$$\beta_k^2\equiv|\langle 1|k\rangle|^2=\frac{\Gamma\Delta/\pi}{(\omega_k-\omega_0)^2+\Gamma^2} \quad (17)$$

with the transmon state, assuming ω_k is close to the resonance, $|\omega_k-\omega_0|\ll\omega_0$ [33]. In new variables, Hamiltonian (16) then reads

$$H_{\rm eff}=\sum_{k>p_c}\omega_k|k\rangle\langle k|+\sum_{0<p<p_c}\omega_p a_p^\dagger a_p+H_1,$$
$$H_1=\lambda_1\sum_{k,k'>p_c}\beta_k\beta_{k'}|k\rangle\langle k'|\cos(2\pi\tilde{n}). \quad (18)$$

It is the "backaction" of the qubit on the dynamic charge $\tilde{n}$ that leads to the emission of "soft" photon modes by the resonant ones [34]. Using Eq. (18), we apply Fermi's golden rule to calculate the (quasielastic) fluorescence spectrum perturbatively in λ_1,

$$\gamma_{\rm si}(\omega_{k'}|\omega_k)=\frac{2\pi^2}{\Delta^2}\sum_f|\langle k',f|H_1|k,0\rangle|^2\delta(\omega_k-\omega_{k'}-E_f). \quad (19)$$

Here $|k,f\rangle=|k\rangle\otimes|f\rangle$ and $|f\rangle$ is a multiphoton state with energy E_f formed out of low-frequency photon modes. By standard manipulations, we express Eq. (19) in terms of a photon correlation function for an array disconnected from a transmon,

$$\gamma_{\rm si}(\omega'|\omega)=\frac{\lambda_1^2\Gamma^2/\pi}{[(\omega-\omega_0)^2+\Gamma^2][(\omega'-\omega_0)^2+\Gamma^2]}\mathcal{C}(\omega-\omega'), \tag{20}$$

with

$$\mathcal{C}(\Omega)=2\mathrm{Re}\int_0^\infty dt e^{i(\Omega+i0^+)t}\langle\cos 2\pi\tilde{n}(t)\cos 2\pi\tilde{n}(0)\rangle. \tag{21}$$

Here $\tilde{n}(t)=(1/\pi)\sum_{0<p<p_c}f_p(a_pe^{-i\omega_pt}+a_p^\dagger e^{i\omega_pt})$. We use extensively Baker-Hausdorff formula [37] to find

$$\mathcal{C}(\Omega)=2e^{-4\sum_p f_p^2}\mathrm{Re}\int_0^\infty dt e^{i(\Omega+i0^+)t}\cosh\left(4\sum_p f_p^2e^{-i\omega_pt}\right) \tag{22}$$

at zero temperature. The Taylor expansion of the cosh factor in Eq. (22) allows interpreting Eq. (20) as a partial cross section of a high-frequency photon scattering into another high-frequency photon, while an even number of low-frequency photons is produced. At $K\to 0$, Eq. (20) reproduces Eq. (13) upon the renormalization [38] of the phase slip amplitude, $\lambda_1\to\lambda_1e^{-2\sum_p f_p^2}\approx\lambda_1(\Delta/\omega_0)^{2K}$, and not too close to the resonance, $\Gamma\ll|\omega-\omega_0|$, $|\omega'-\omega_0|\ll\omega_0$.

Being proportional to $\lambda_1^2(\Delta/\omega_0)^{4K}$, the three-photon amplitude vanishes in the thermodynamic limit at finite K. Thus higher-order processes should be included. Instead of evaluating and summing them we note that at $\Delta\to 0$ Eq. (21) can be simplified,

$$\mathcal{C}(\Omega)\approx\mathrm{Re}\int_0^\infty dt e^{i(\Omega+i0^+)t}\langle e^{i2\pi\tilde{n}(t)}e^{-i2\pi\tilde{n}(0)}\rangle. \tag{23}$$

This correlator has been much studied [5,39],

$$\mathcal{C}(\Omega)=\frac{\pi}{\Gamma(4K)}\frac{1}{\Omega}\left(\frac{\Omega}{\omega_0}\right)^{4K}e^{-\Omega/\omega_0},\qquad \Omega>0. \tag{24}$$

Here $\Gamma(4K)$ is the Gamma function. Equation (20) with $\mathcal{C}(\Omega)$ of Eq. (24) is our main result [40]. It relates the fluorescence spectrum with the dynamical phase-boost susceptibility $\propto\mathcal{C}(\omega)$ at $\omega\ll\omega_0$ [3] in the same range of validity defined by Eq. (1).

Inserting Eq. (24) in Eq. (20) we find that at resonant excitation, $|\omega-\omega_0|\lesssim\Gamma$, and in the frequency range $\omega_0\gg\omega_0-\omega'\gg\Gamma$ of the emitted photons, the fluorescence intensity is a power law [41] of $\omega_0-\omega'$,

$$\gamma_{\rm si}(\omega'|\omega)=\frac{1}{\Gamma(4K)}\frac{\lambda_1^2}{\omega_0^3}\left(\frac{\omega_0-\omega'}{\omega_0}\right)^{4K-3}. \tag{25}$$

The perturbative-in-λ_1 result for the differential cross-section of quasielastic scattering works at any K, except its smallest values allowing for $\lambda_1\gtrsim\Gamma$. The behavior of Eq. (25) parallels the one of the dynamical susceptibility $A(\omega)$ of Eq. (10) in Ref. [42]. These two quantities are not normalizable at $K<1/2$, which is the signature of the charge localized phase. At the critical point ($K=1/2$), we find $\gamma(\omega'|\omega_0)\propto 1/(\omega_0-\omega')$ as the dynamical critical signature of the Schmid transition.

Total inelastic cross section.—Finally, we show that at $K<1/2$ the quasielastic transitions may yield the main contribution to the *total* inelastic cross section [43],

$$\gamma(\omega)=\int_0^\omega d\omega'\gamma(\omega'|\omega). \tag{26}$$

Indeed, at $K<1/2$ the dominant contribution of the partial cross section (20) to the integral comes from a vicinity of order Γ near its upper bound. We may thus extend the lower bound in Eq. (26) to $-\infty$ and evaluate the quasielastic component of the total cross section as

$$\gamma_{\rm si}(\omega_0)=\frac{\pi}{2\sin(2\pi K)\Gamma(4K)}\frac{\lambda_1^2}{\Gamma^2}\left(\frac{\Gamma}{\omega_0}\right)^{4K} \tag{27}$$

for the incoming photons lying within the width of the resonance. Furthermore, the inelastic spectral linewidth is asymmetric, see Fig. 2, with asymptotes

$$\gamma_{\rm si}(\omega)=\frac{\pi\lambda_1^2\Gamma/\omega_0^3}{\Gamma(4K)}\left(\frac{\omega_0}{\omega-\omega_0}\right)^{3-4K} \tag{28}$$

at $\omega-\omega_0\gg\Gamma$ and

$$\gamma_{\rm si}(\omega)=\frac{\pi(1-4K)\lambda_1^2\Gamma^2/\omega_0^4}{\sin(4\pi K)\Gamma(4K)}\left(\frac{\omega_0}{\omega_0-\omega}\right)^{4-4K} \tag{29}$$

at $\omega_0-\omega\gg\Gamma$. Importantly, the found $\gamma_{\rm si}(\omega)$ is independent of the artificially-introduced partition frequency ω_c thus justifying the use of Eq. (16).

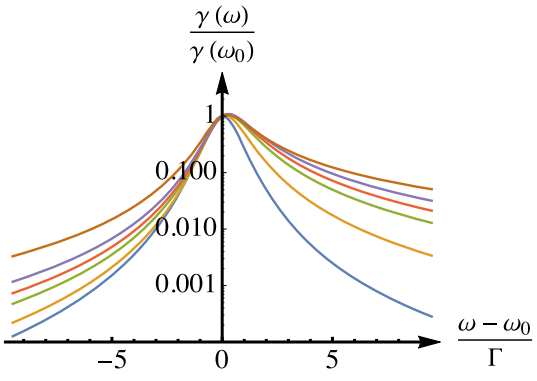

FIG. 2. Frequency dependence of the total cross section at zero temperature for $K=0.01$ (blue), 0.1 (orange), 0.2 (green), 0.25 (red), 0.3 (purple), and 0.4 (brown).

To assess the contribution to Eq. (26) of deeply inelastic processes, we use the differential cross section (14) stemming from the transmon anharmonicity and favoring large energy transfer between the incoming and any of the outgoing photons. The corresponding contribution to the total cross section is

$$\gamma_{\rm q}(\omega_0) = \alpha \frac{\Gamma^2 \tilde{E}_C^2}{\omega_0^4} \quad \text{with} \quad \alpha \approx 0.45. \tag{30}$$

The comparison with Eq. (27) shows that quasielastic processes dominate the total inelastic cross section $\gamma(\omega)$ if $\lambda_1/\tilde{E}_C \gg (\Gamma/\omega_0)^{2(1-K)}$. Under the assumption $\lambda_1 \ll \Gamma$, this condition is possible to satisfy only at $K < 1/2$: in terms of the Schmid transition, the phase-slip mechanism may dominate the total inelastic cross section only in the charge-localized phase.

While Eqs. (20) and (24) remain valid at $K > 1/2$, their use in evaluation of $\gamma(\omega)$ is not justified: the dominant contribution to the integral in Eq. (26) at $K > 1/2$ comes from $\omega - \omega' \gtrsim \omega_c$ and depends on ω_c, rendering the model (16) inapplicable. This is consistent with our perturbative analysis of Eq. (5): there is no parameter allowing to single out the phase-slip-induced transitions from other processes at energy losses comparable to ω_0.

It is straightforward to generalize Eqs. (20) and (27)–(29) to finite temperatures T, by using the corresponding finite-T generalization [5,39] of $\mathcal{C}(\Omega)$. A low temperature, $T \ll \omega_0$, leaves the power-law spectrum (25) intact at $\omega_0 - \omega' \gg T$. The total inelastic cross-section in the scaling region $[\Gamma, |\omega - \omega_0|, T \ll \omega_0]$ is found as

$$\frac{\gamma(\omega, T)}{\gamma(\omega_0, 0)} = \frac{\sin(2\pi K)}{\pi^2} \frac{\tau^{4K-1}}{1+\nu^2} \int_0^\infty dx \frac{e^{\pi x/\tau} |\Gamma(2K + ix/\tau)|^2}{(x-\nu)^2 + 1}, \tag{31}$$

with $\tau = 2\pi T/\Gamma$ and $\nu = (\omega - \omega_0)/\Gamma$. Its temperature dependence at resonance, $\omega = \omega_0$, is shown in Fig. 3. The total cross section increases (decreases) with the temperature at $K > 1/4$ ($K < 1/4$). At low temperature $T \ll \Gamma$,

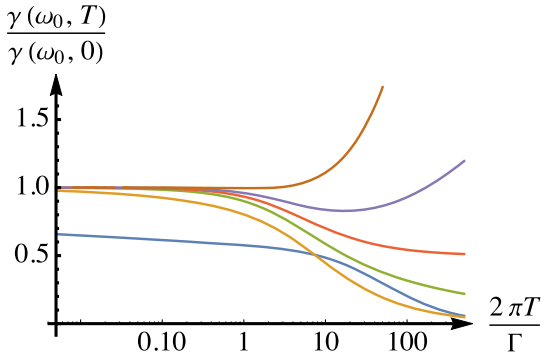

FIG. 3. Temperature dependence of the total cross section at resonance (same color code as in Fig. 2).

$$\frac{\gamma(\omega_0, T)}{\gamma(\omega_0, 0)} \approx 1 - \frac{1}{2}\left(\frac{2\pi T}{\Gamma}\right)^{4K}, \tag{32}$$

where the second term is a significant correction in a wide temperature range at $K \ll 1$.

Conclusion.—We believe the spectrum of the fluorescence that we predict, see Eqs. (20)–(25), charts an interesting direction for future experiments, while the found total inelastic cross section, see Eqs. (26)–(32), is directly related to the ongoing experiments [44] in the spirit of Refs. [16–18]. Indeed, the internal quality factor $Q(\omega)$ of a discrete mode in a finite-length array, which is routinely measured in such experiments, can be expressed in terms of an inelastic decay rate, $Q(\omega) = \omega/\Gamma_{\rm in}(\omega)$. The latter is related to the total inelastic cross section through $\Gamma_{\rm in}(\omega) = \gamma(\omega)\Delta/\pi$. Lastly, in the weakly nonlinear transmon regime, which we focussed upon, photon scattering remains mostly elastic. As the nonlinearity increases, we may anticipate large inelastic cross sections, which would manifest a different kind of quantum impurity problem than the Kondo regime studied in Refs. [20,21].

We acknowledge stimulating discussions with M. Goldstein and with V. Manucharyan who attracted our attention to the role of phase slips, as well as B. Beri and N. Roch for useful comments on the manuscript. This work is supported by the DOE Contract No. DE-FG02-08ER46482 (L. G.), and by ANR through Grant No. ANR-16-CE30-0019 and ARO Grant No. W911NF-18-1-0212 (M. H.).

[1] A. Schmid, Phys. Rev. Lett. **51**, 1506 (1983).
[2] S. A. Bulgadaev, Pis'ma Zh. Eksp. Teor. Fiz. **39**, 264 (1984) [JETP Lett. **39**, 315 (1984)], http://www.jetpletters.ac.ru/ps/1289/article_19477.shtml.
[3] F. Guinea, V. Hakim, and A. Muramatsu, Phys. Rev. Lett. **54**, 263 (1985).
[4] M. P. A. Fisher and W. Zwerger, Phys. Rev. B **32**, 6190 (1985).
[5] G. Schön and A. D. Zaikin, Phys. Rep. **198**, 237 (1990).
[6] R. Yagi, S. I. Kobayashi, and Y. Ootuka, J. Phys. Soc. Jpn. **66**, 3722 (1997).
[7] J. S. Penttilä, P. J. Hakonen, E. B. Sonin, and M. A. Paalanen, J. Low Temp. Phys. **125**, 89 (2001).
[8] M. Watanabe and D. B. Haviland, Phys. Rev. B **67**, 094505 (2003).
[9] A. Murani, N. Bourlet, H. le Sueur, F. Portier, C. Altimiras, D. Esteve, H. Grabert, J. Stockburger, J. Ankerhold, and P. Joyez, Phys. Rev. X **10**, 021003 (2020).
[10] Let us clarify that the fluorescence considered here can be studied at weak ac drive; it differs from the resonance fluorescence of a strongly driven qubit [11] resulting in the appearance of Mollow triplet in the spectrum.
[11] O. Astafiev, A. M. Zagoskin, A. A. Abdumalikov, Y. A. Pashkin, T. Yamamoto, K. Inomata, Y. Nakamura, and J. S. Tsai, Science **327**, 840 (2010).

[12] J. Koch, T. M. Yu, J. Gambetta, A. A. Houck, D. I. Schuster, J. Majer, A. Blais, M. H. Devoret, S. M. Girvin, and R. J. Schoelkopf, Phys. Rev. A **76**, 042319 (2007).

[13] J. A. Schreier, A. A. Houck, J. Koch, D. I. Schuster, B. R. Johnson, J. M. Chow, J. M. Gambetta, J. Majer, L. Frunzio, M. H. Devoret, S. M. Girvin, and R. J. Schoelkopf, Phys. Rev. B **77**, 180502(R) (2008).

[14] N. A. Masluk, I. M. Pop, A. Kamal, Z. K. Minev, and M. H. Devoret, Phys. Rev. Lett. **109**, 137002 (2012).

[15] M. T. Bell, I. A. Sadovskyy, L. B. Ioffe, A. Yu. Kitaev, and M. E. Gershenson, Phys. Rev. Lett. **109**, 137003 (2012).

[16] J. Puertas Martínez, S. Léger, N. Gheeraert, R. Dassonneville, L. Planat, F. Foroughi, Y. Krupko, O. Buisson, C. Naud, W. Hasch-Guichard, S. Florens, I. Snyman, and N. Roch, npj Quantum Inf. **5**, 19 (2019).

[17] R. Kuzmin, N. Mehta, N. Grabon, R. Mencia, and V. E. Manucharyan, npj Quantum Inf. **5**, 20 (2019).

[18] S. Léger, J. Puertas-Martínez, K. Bharadwaj, R. Dassonneville, J. Delaforce, F. Foroughi, V. Milchakov, L. Planat, O. Buisson, C. Naud, W. Hasch-Guichard, S. Florens, I. Snyman, and N. Roch, Nat. Commun. **10**, 5259 (2019).

[19] J. J. García-Ripoll, E. Solano, and M. A. Martin-Delgado, Phys. Rev. B **77**, 024522 (2008).

[20] K. Le Hur, Phys. Rev. B **85**, 140506(R) (2012).

[21] M. Goldstein, M. H. Devoret, M. Houzet, and L. I. Glazman, Phys. Rev. Lett. **110**, 017002 (2013).

[22] I. Snyman and S. Florens, Phys. Rev. B **92**, 085131 (2015).

[23] N. Gheeraert, X. H. H. Zhang, T. Sépulcre, S. Bera, N. Roch, H. U. Baranger, and S. Florens, Phys. Rev. A **98**, 043816 (2018).

[24] T. Yamamoto and T. Kato, J. Phys. Soc. Jpn. **88**, 094601 (2019).

[25] F. W. J. Hekking and L. I. Glazman, Phys. Rev. B **55**, 6551 (1997).

[26] R. M. Bradley and S. Doniach, Phys. Rev. B **30**, 1138 (1984).

[27] S. E. Korshunov, Zh. Eksp. Teor. Fiz. **95**, 1058 (1989) [Sov. Phys. JETP **68**, 609 (1989)], http://www.jetp.ac.ru/cgi-bin/e/index/e/68/3/p609?a=list.

[28] D. M. Basko, F. Pfeiffer, P. Adamus, M. Holzmann, and F. W. J. Hekking, Phys. Rev. B **101**, 024518 (2020).

[29] V. Manucharyan (private communication).

[30] A. O. Gogolin, A. A. Nersesyan, and A. M. Tsvelik, *Bosonization and Strongly Correlated Systems* (Cambridge University Press, Cambridge, England, 1998).

[31] Equation (10) is reminiscent of a famous expression for the effective mass tensor in Bloch band theory, see Eq. (59.5) in [E. M. Lifshitz and L. P. Pitaevskii, *Statistical Physics, Part 2: Theory of the Condensed State* (Pergamon Press, Oxford, 1980)].

[32] In Eq. (16) we dispense with the term $-\lambda_0|0\rangle\langle 0|\cos(2\pi\tilde{n})$, which is responsible for charge localization in the ground state ($\lambda_0 \ll \lambda_1$).

[33] The density of states (DOS), $(1/\pi)dk/d\omega_k$, contains a Lorentzian peak corresponding to the resonant level. In a finite chain, it translates into a nonequidistant spectrum ω_k, making the DOS width 2Γ an experimentally accessible parameter [17].

[34] The resonance renders the effect of phase slips on inelastic scattering markedly different from the one considered in homogeneous Josephson-junction chains [35,36].

[35] M. Bard, I. V. Protopopov, and A. D. Mirlin, Phys. Rev. B **98**, 224513 (2018).

[36] M. Houzet and L. I. Glazman, Phys. Rev. Lett. **122**, 237701 (2019).

[37] $e^A e^B = e^{A+B} e^{(1/2)[A,B]}$ when $[A, B]$ is a c number.

[38] In this limit, the intermediate scale ω_c can be replaced with ω_0, and thus drops from the result.

[39] U. Weiss and H. Grabert, Phys. Lett. **108A**, 63 (1985).

[40] Equation (20) also holds at finite λ_0 provided that the quantum average in $\mathcal{C}(\Omega)$ is performed with $H_{\rm sG}$. At $K < 1/2$, standard methods yield $\mathcal{C}(\Omega \ll \omega_\star) \propto \Omega/\omega_\star^2$ with the soft gap $\omega_\star \sim \omega_0(\lambda_0/\omega_0)^{1/(1-2K)}$ [30]. Thus charge localization in the ground state is unveiled by the suppression of $\gamma_{\rm si}$ at small frequency exchange. We safely ignore that structure in our results, as $\omega_\star \ll \Gamma$.

[41] Again, the chosen frequency range allowed us to replace ω_c that was initially appearing in Eq. (24) by ω_0.

[42] F. Guinea, Phys. Rev. B **32**, 4486 (1985).

[43] In Ref. [21] we were invoking energy conservation instead,

$$\omega\gamma(\omega) = \int_0^\omega d\omega' \omega' \gamma(\omega'|\omega). \tag{33}$$

The two formulas agree with each other when quasielastic transitions dominate.

[44] R. Kuzmin, N. Grabon, N. Mehta, A. Burshtein, M. Goldstein, M. Houzet, L. I. Glazman, and V. E. Manucharyan, arXiv:2010.02099.